Phase transformation and room temperature stabilization of various Bi_2O_3 nano-polymorphs: Effect of oxygen-vacancy defects and reduced surface energy due to adsorbed carbon species

Ashish Chhaganlal Gandhi, Chi-Yuan Lai, Kuan-Ting Wu, P. V. R. K. Ramacharyulu, Valmiki B. Koli, Chia-Liang Cheng, Shyue-Chu Ke and Sheng Yun Wu*

Department of Physics, National Dong Hwa University, Hualien 97401, Taiwan

Fig. S1 Rietveld refined PXRD spectra from Bi NPs and annealed samples.
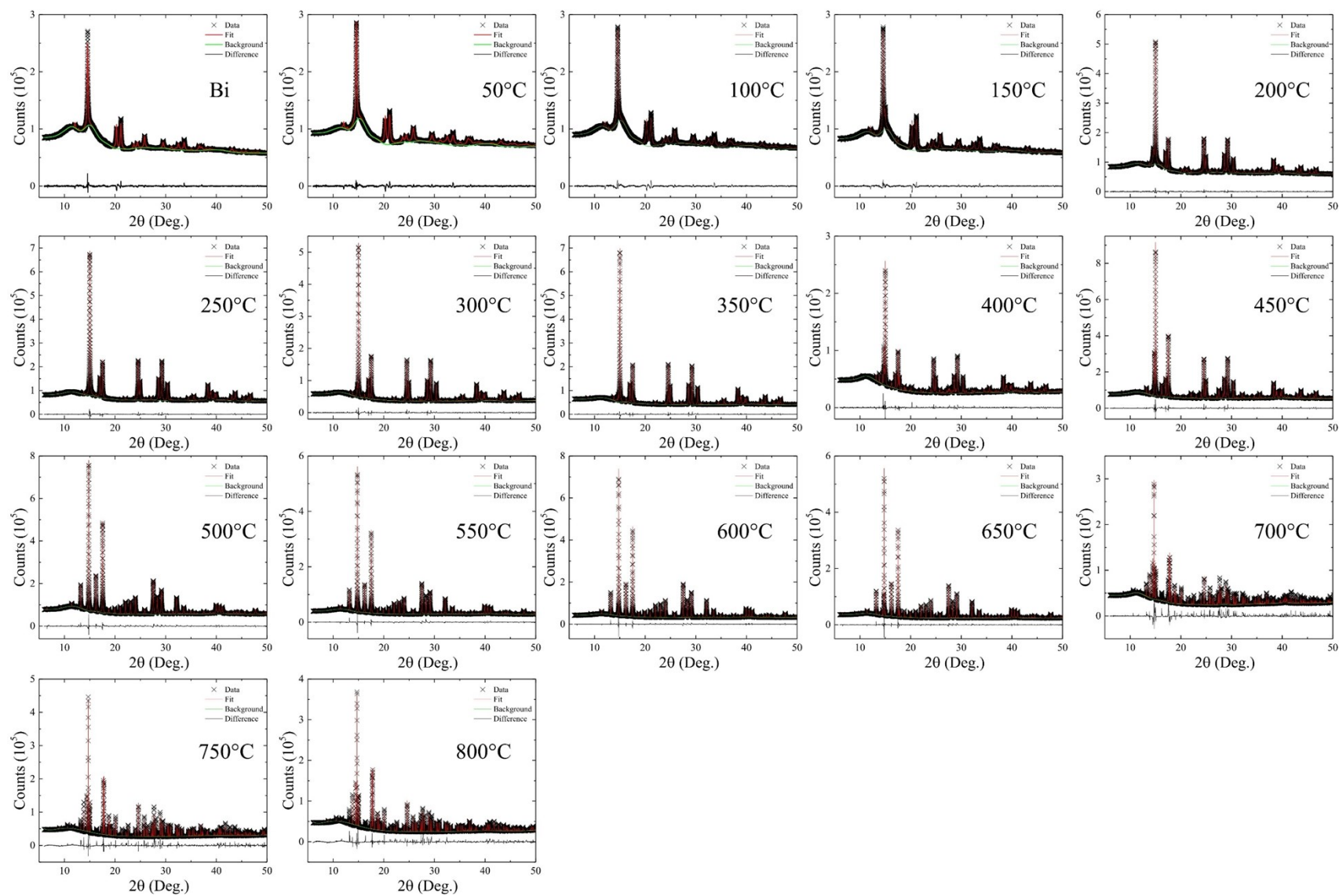
Fig. S2 Annealing temperature T_A dependency of fitted values of lattice constants obtained from (a) Bi, (b) β-Bi$_2$O$_3$, (c) γ-Bi$_2$O$_3$, and (d) α-Bi$_2$O$_3$.
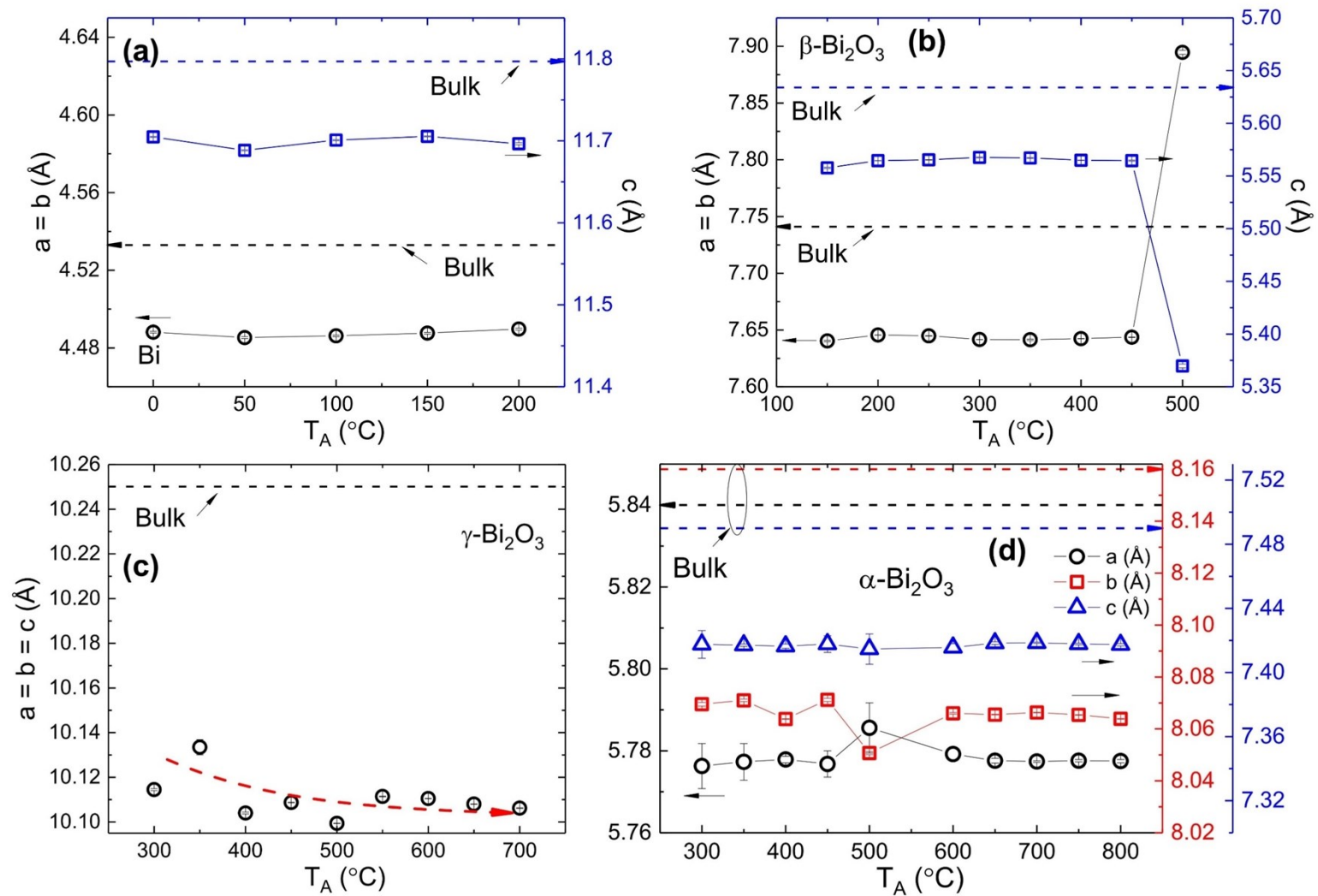
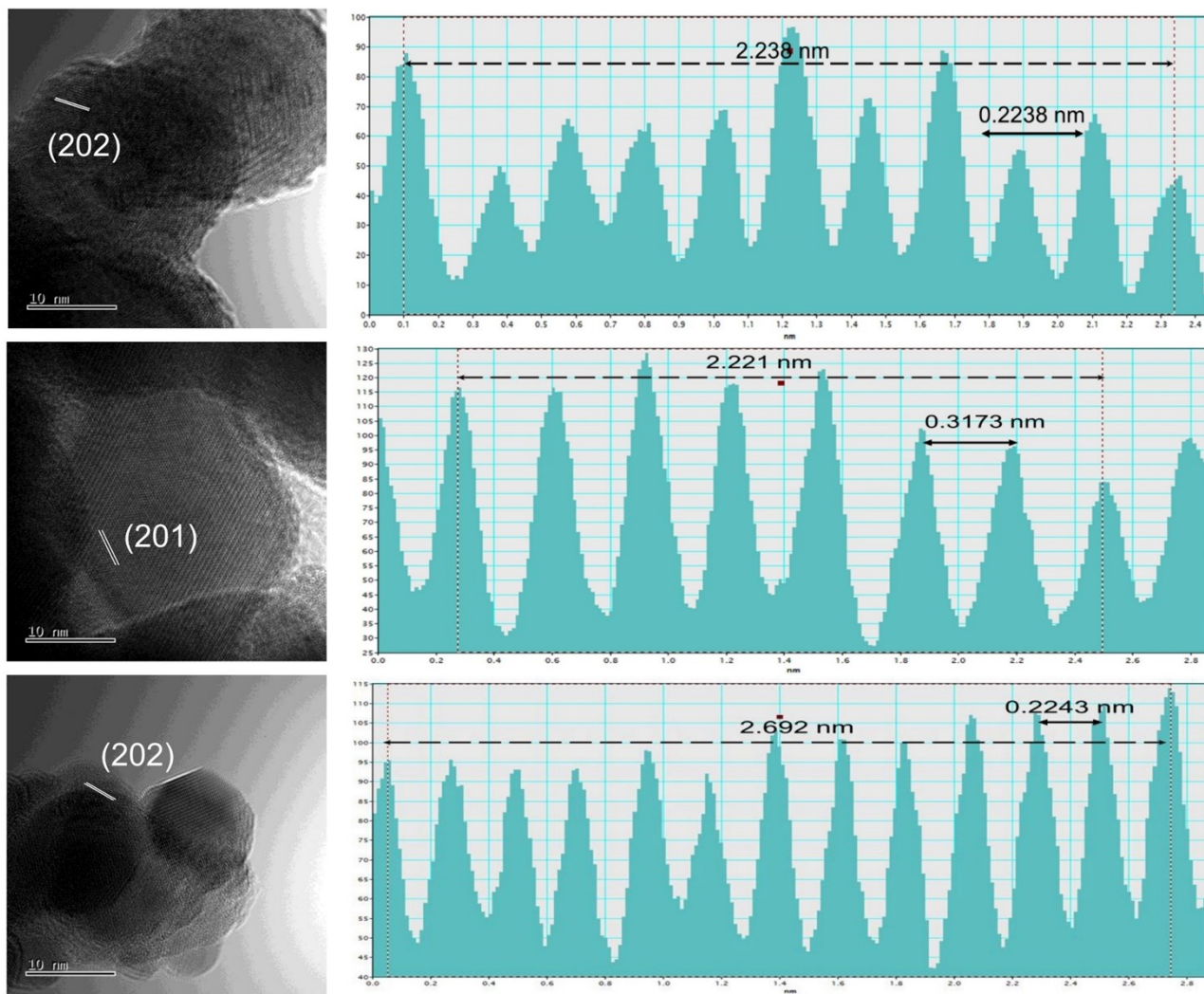**Fig. S3** HRTEM images from β-Bi$_2$O$_3$ NPs.

Fig. S4 HRTEM images from γ-Bi₂O₃ NPs.
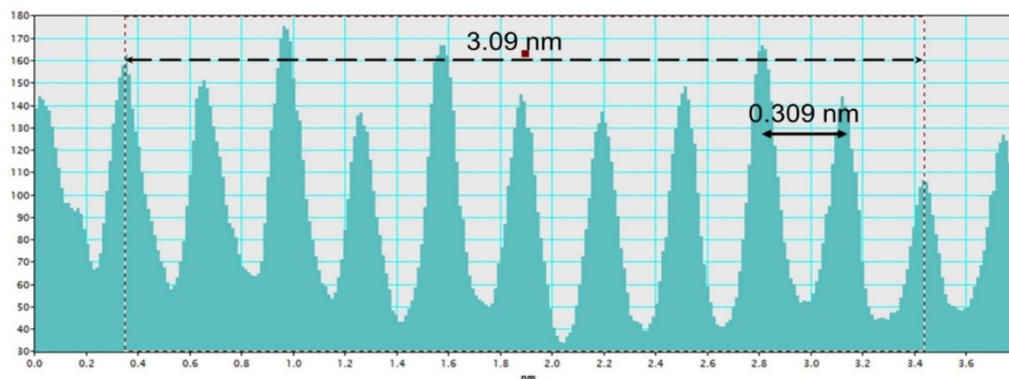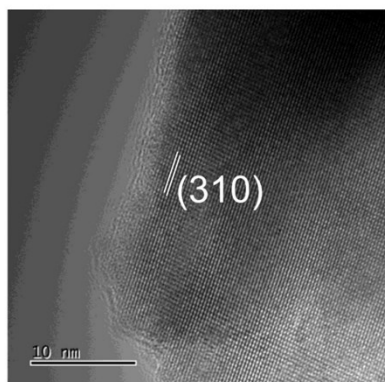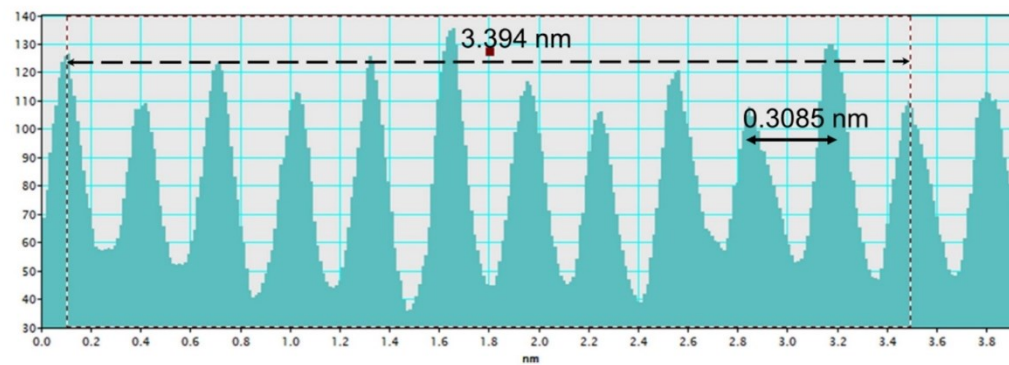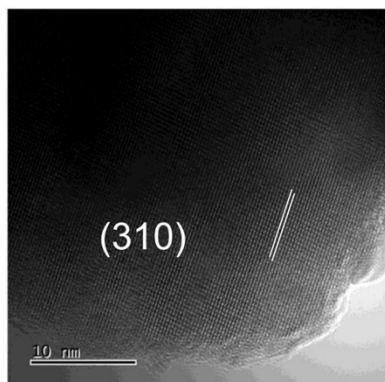
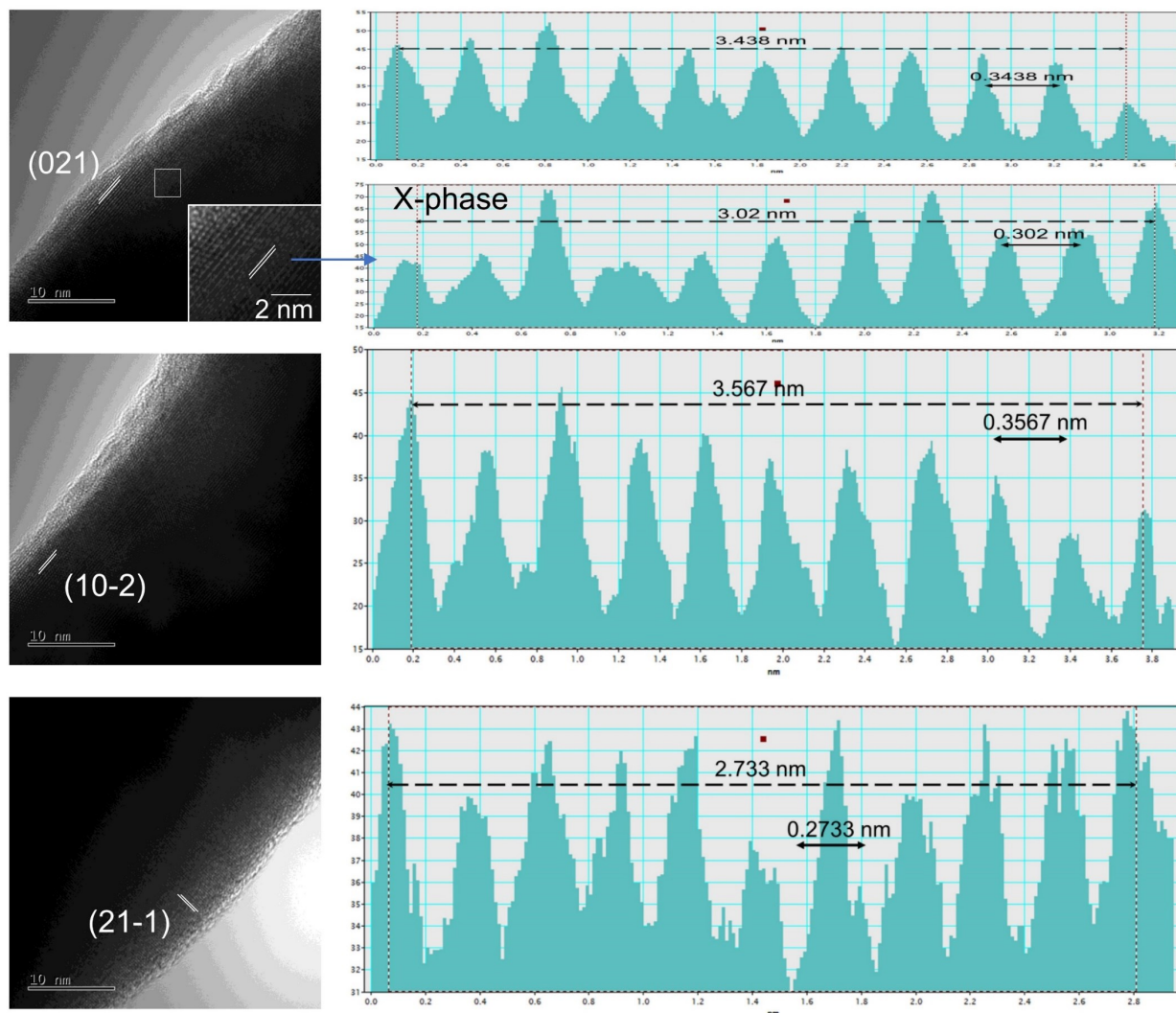**Fig. S5** HRTEM images from α/R-Bi$_2$O$_3$ particles.

Fig. S6 Mean diameter distribution histogram obtained from SEM images of Bi and all annealed samples. The red line represents a fit using the Log-normal distribution function.
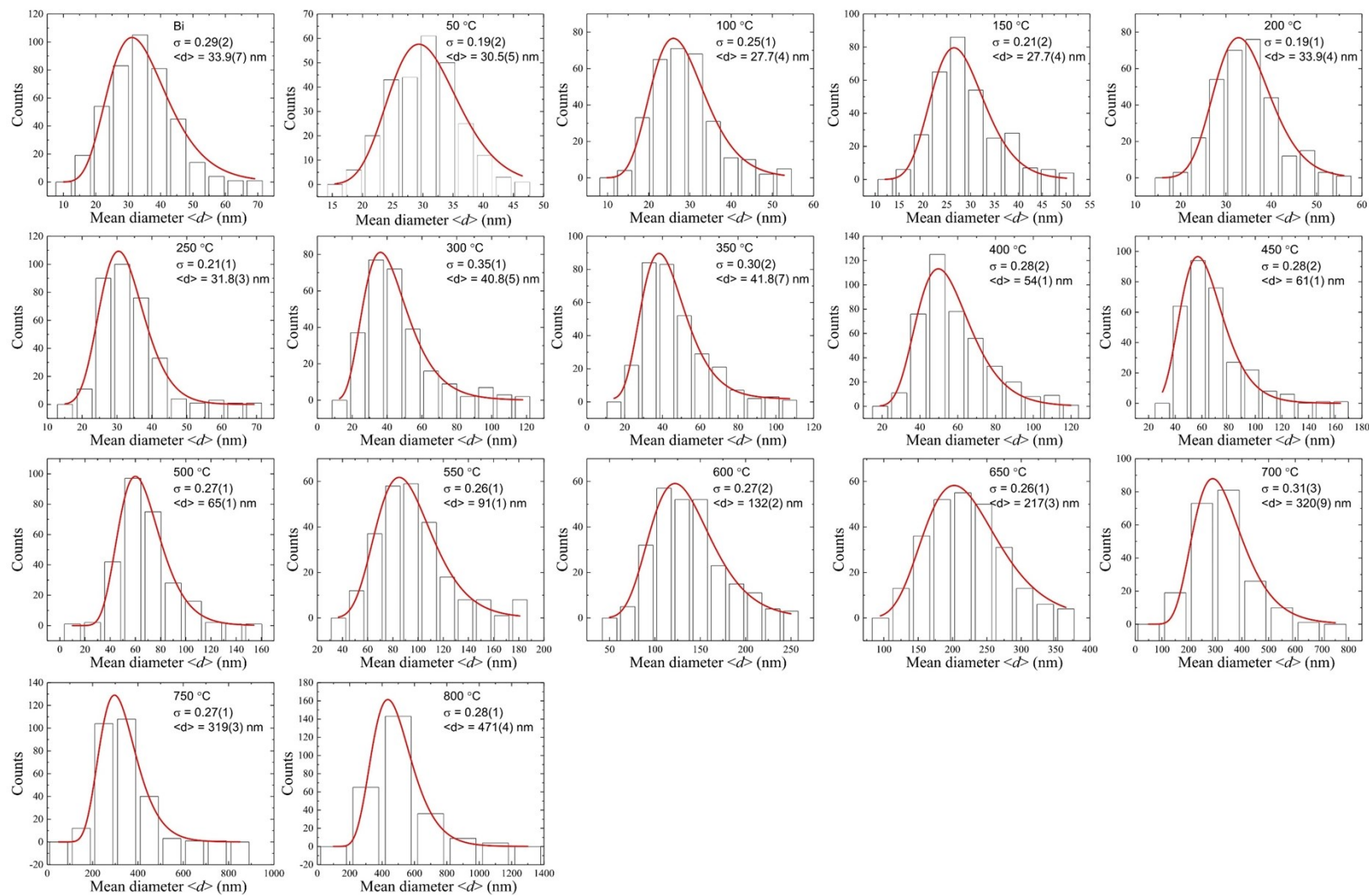
Fig. S7 (a)-(d) Raman spectra obtained from Bi and all annealed samples.
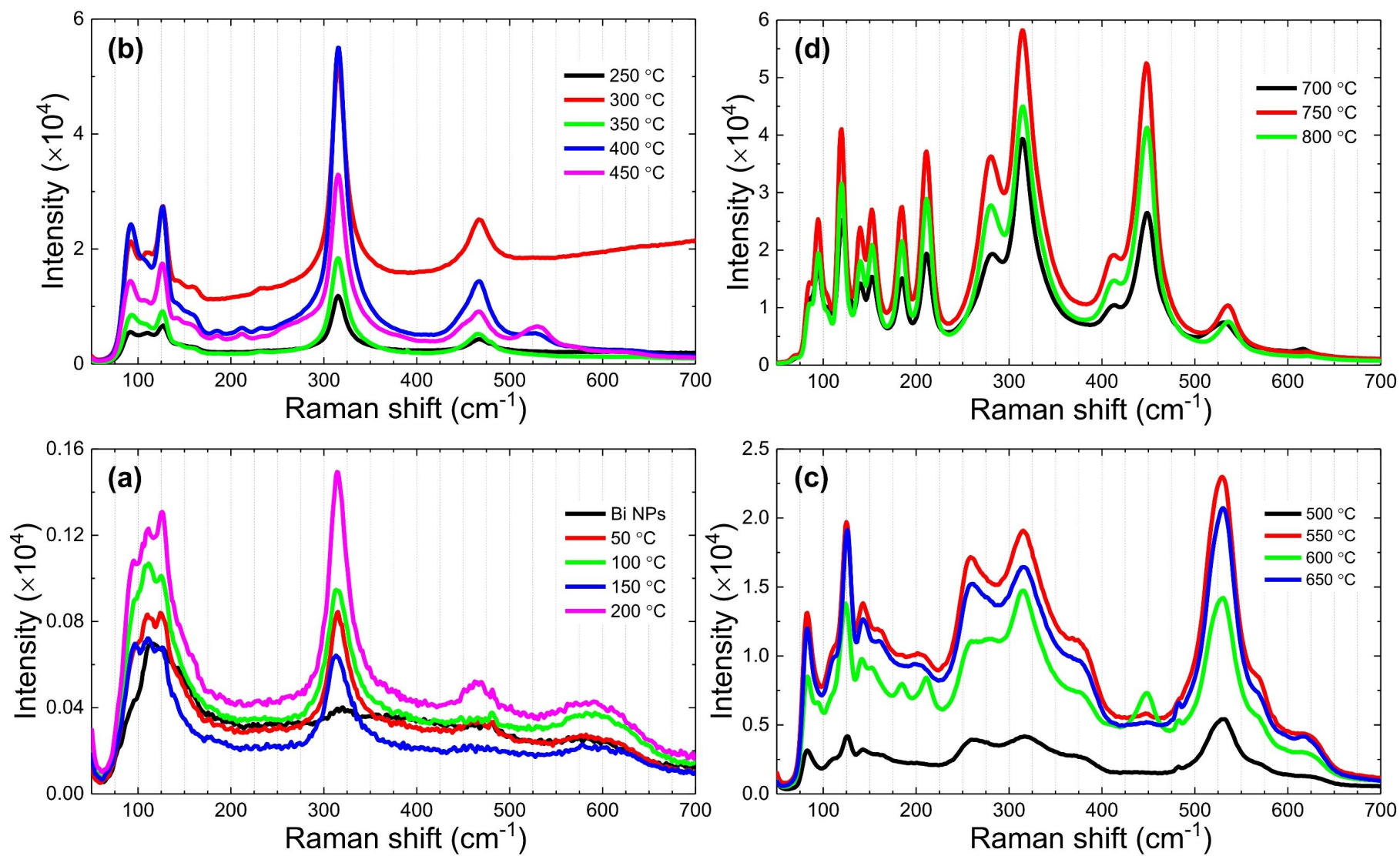
Fig. S8 Photodegradation of methylene blue dye solution using β-Bi$_2$O$_3$ NPs

The photodegradation efficiency of β-Bi$_2$O$_3$ NPs (T$_A$ = 250 °C) was evaluated by photodegradation of the methylene blue (MB) dye aqueous solution. MB degradation was carried out under visible light irradiation by using a 65 W LED bulb. The UV light tubes were placed inside a square box. The 5 ppm MB dye solution with 20 mg of the photocatalyst in a glass beaker was magnetically stirred. The distance between the applied light source and the surface of the MB solution was 15 cm, and the photodegradation study was carried out at room temperature. To ensure the adsorption-desorption equilibrium, the whole suspension was magnetically stirred in the dark for 30 min at room temperature. Then the solution was irradiated with a LED light source. At the regular time interval, 3 ml of aliquots were withdrawn from the suspension and centrifuged immediately to separate the photocatalyst. The photodegradation change in the concentration of MB dye in the solution was analyzed using a UV-vis spectrometer (Spectra Academy, SV2100) by measuring the absorbance in the wavelength range 500–750 nm, while double distilled water is used as a reference (**Figure S5(a)**). The normalized temporal concentration changes (C$_t$/C$_0$ where C$_0$ is the initial concentration of MB and C$_t$ at the irradiation time t) of MB dye recorded during the photocatalytic process are proportional to the normalized integrated area of the absorbance curve, and it can be obtained from the change in the MB dye absorption profile at a given time interval (**Figures S5(b)**). β-Bi$_2$O$_3$ NPs exhibited 19.06 % photodegradation of MB dye after 360 min of LED light irradiation, consistent with the literature.[1]
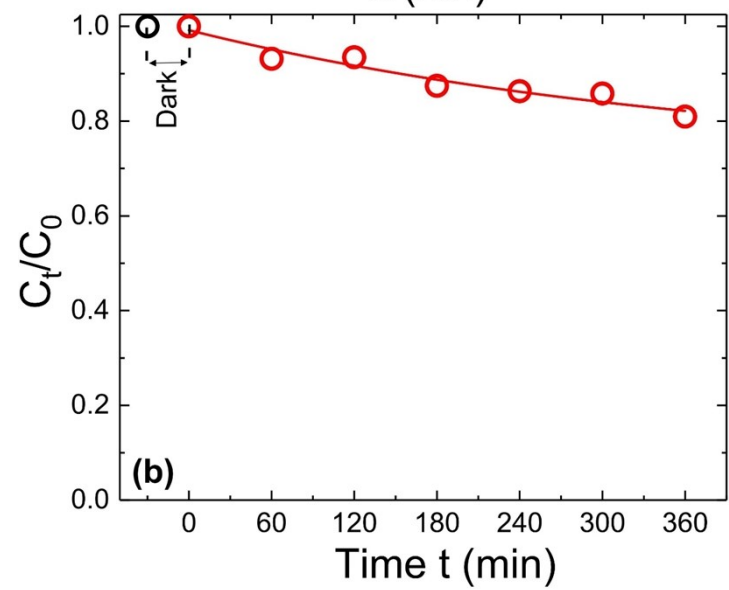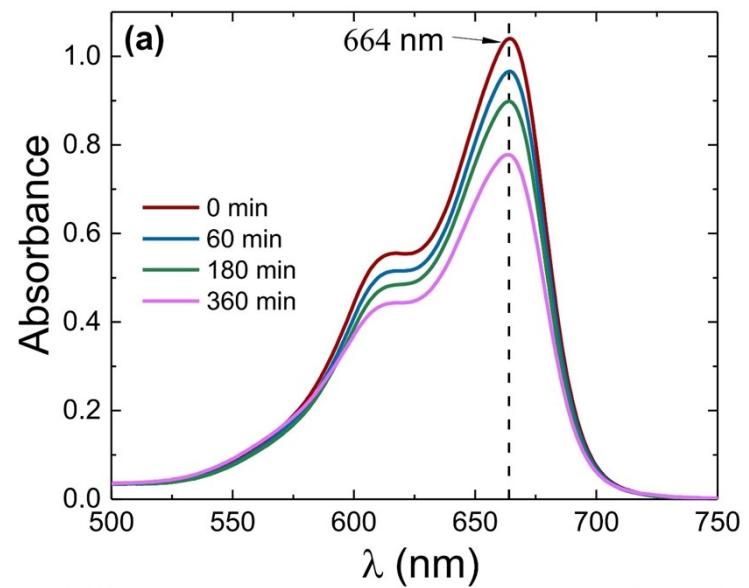
Fig. S9 Deconvoluted PL spectra obtained from Bi and all annealed samples.
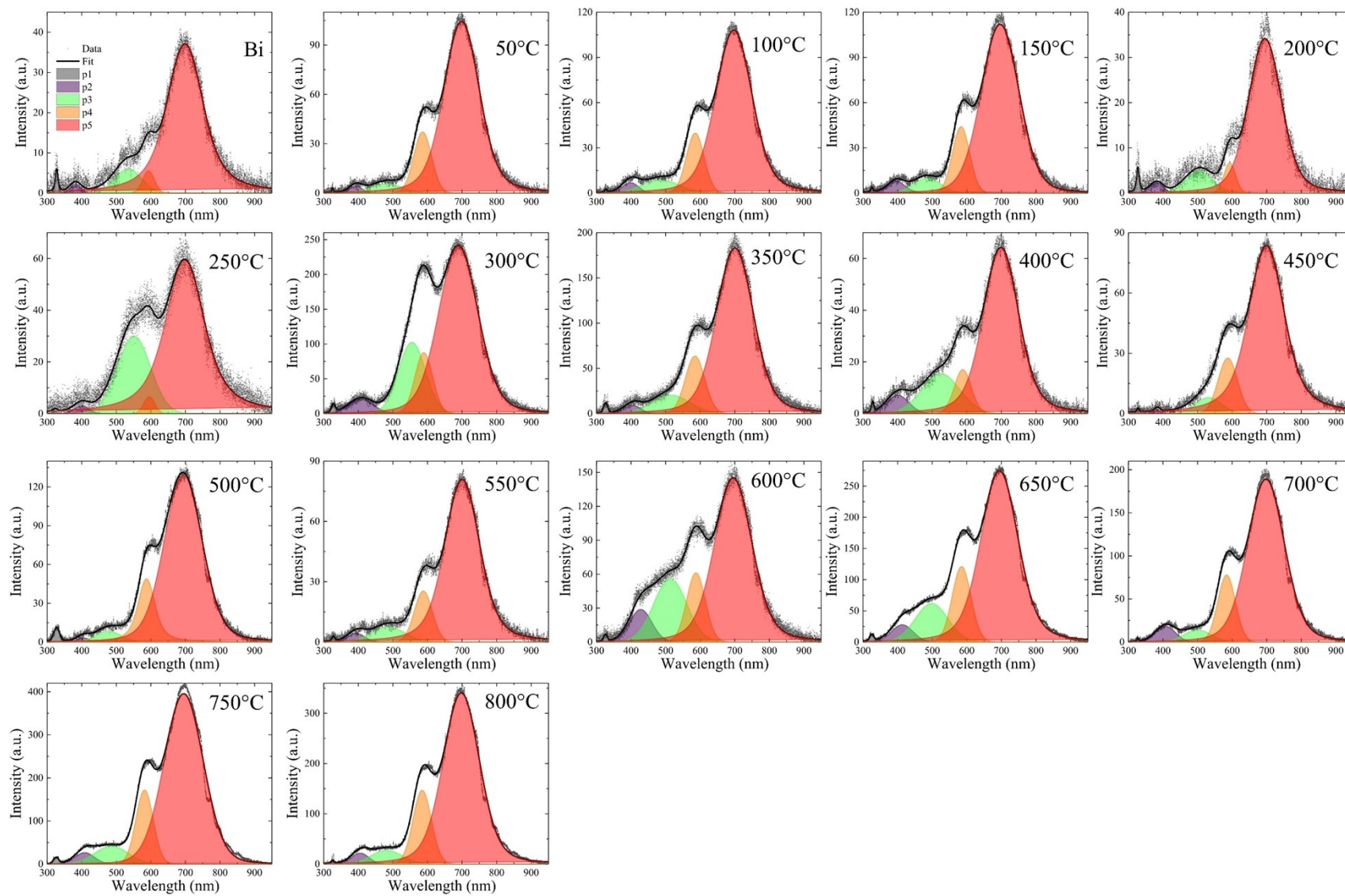
Fig. S10 Plot of annealing temperature T_A dependency of the integrated area of various peaks obtained from PL spectra.
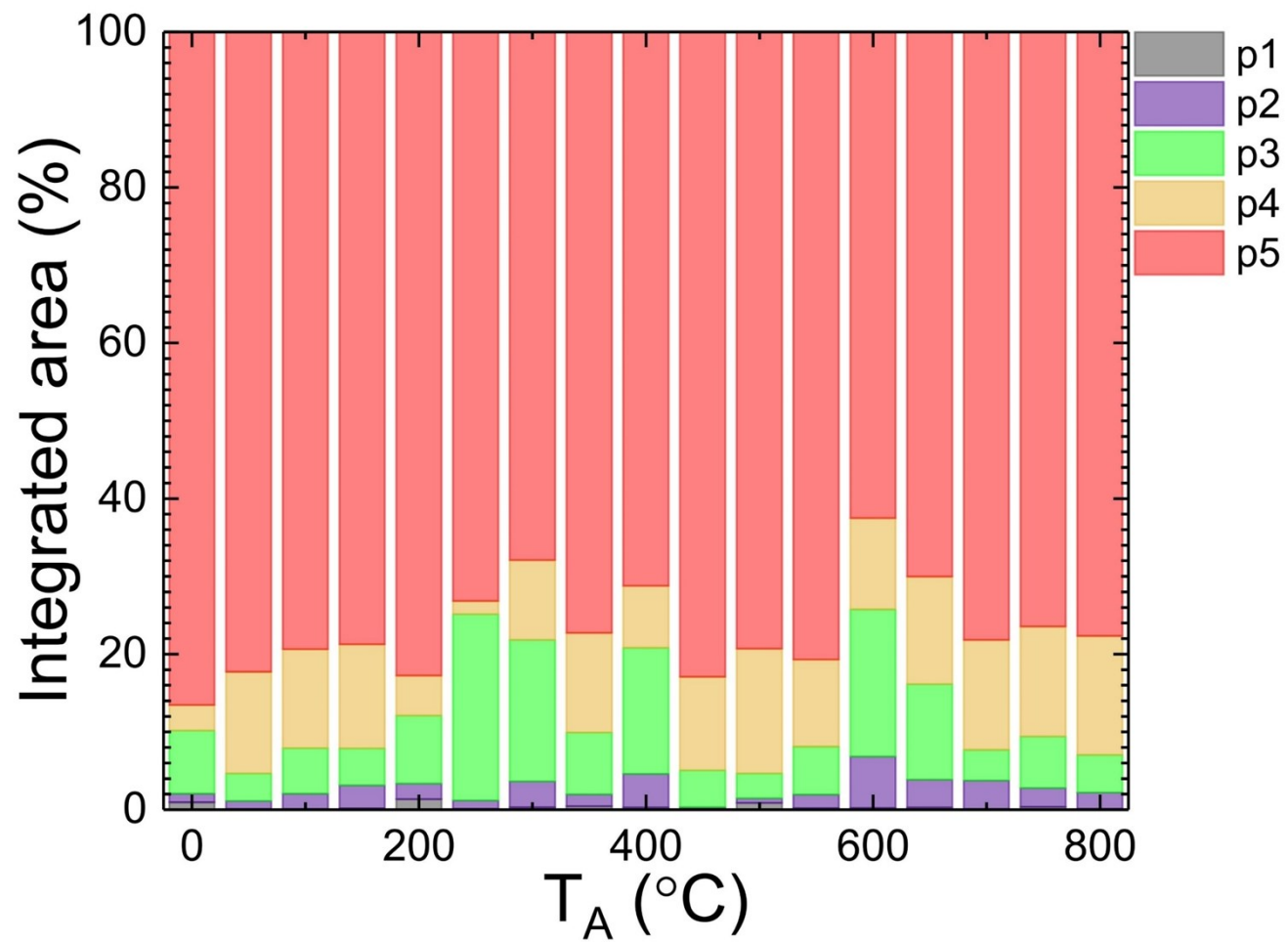
Fig. S11 Plot of PL emission spectra obtained from pure and the air annealed Bi ingots at various temperatures depicted in the figure.
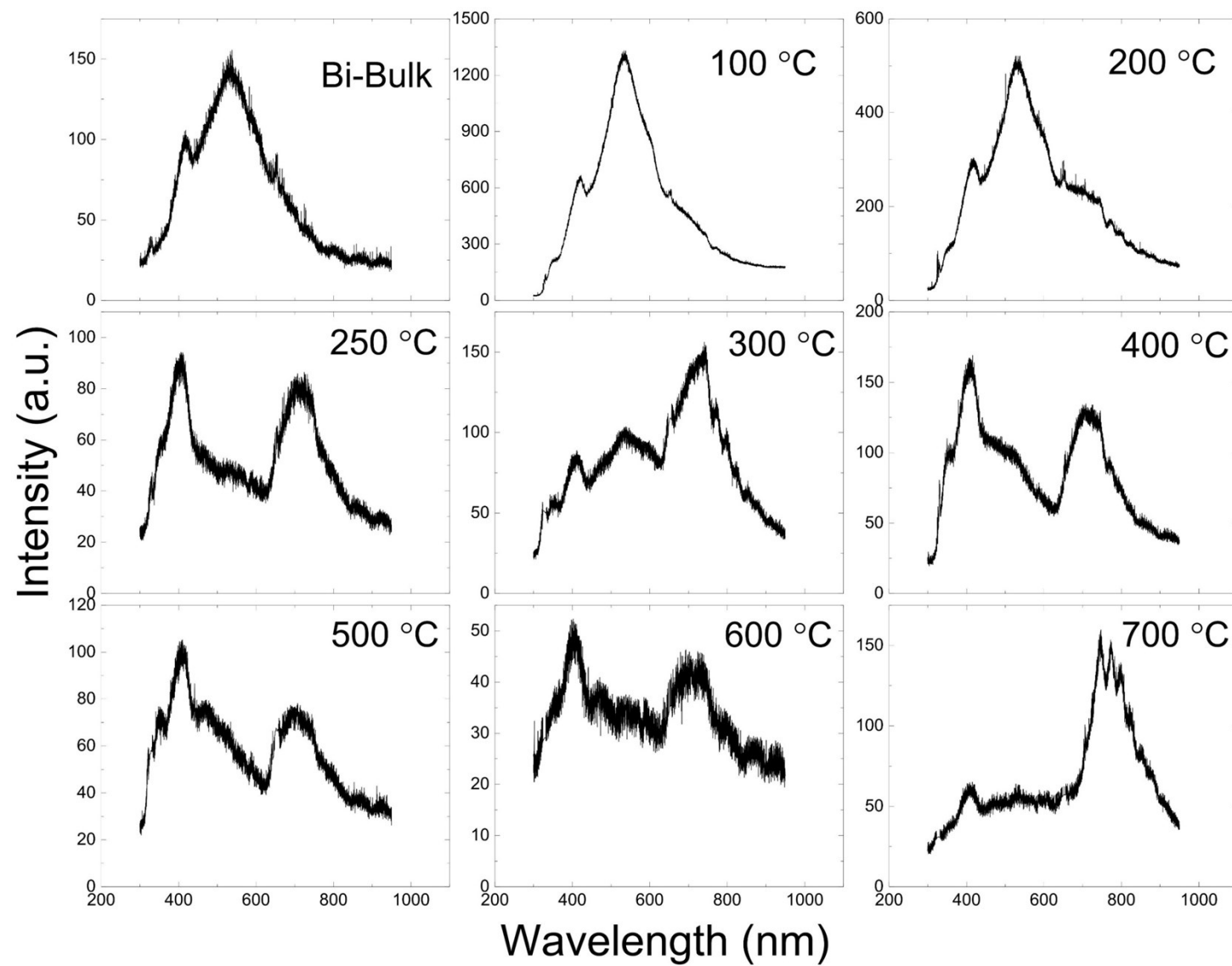
Fig. S12 Annealing temperature T_A dependency of (a) CIE (X, Y) coordinates and (b) CCT obtained from PL spectra of the pure and air annealed Bi NPs (solid dots) and ingots (open dots).
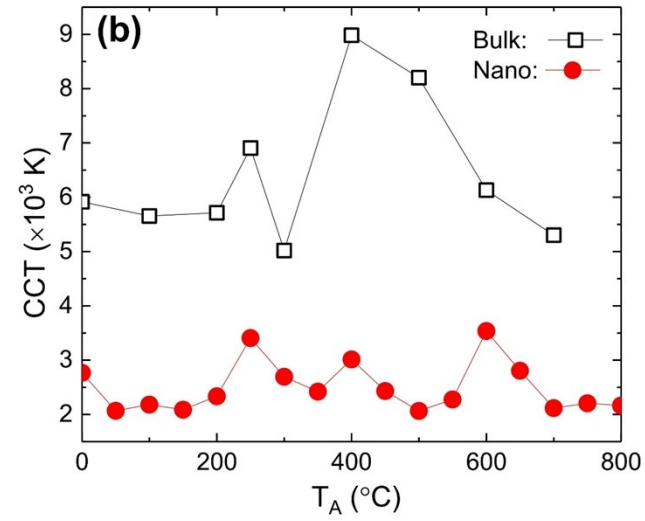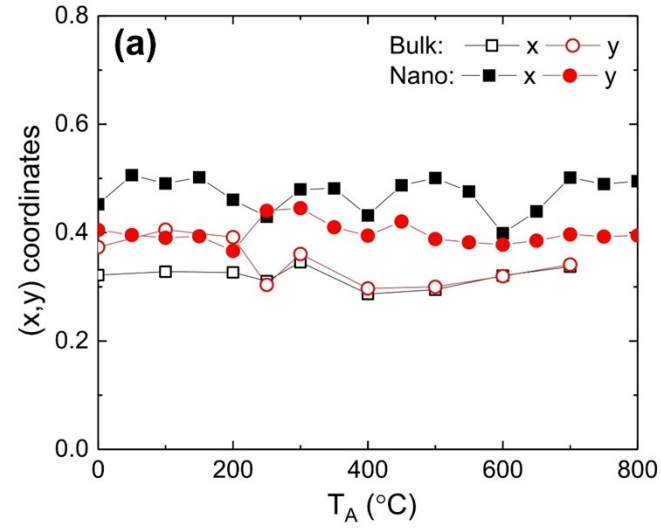
Fig. S13 (a) Magnetic hysteresis loop measured at 1.8 K from pure and the air annealed Bi NPs. (b) Annealing temperature T_A dependency of the estimated value of DC magnetic susceptibility (χ) from pure and the air annealed Bi NPs, where the solid red line is guided for eyes.
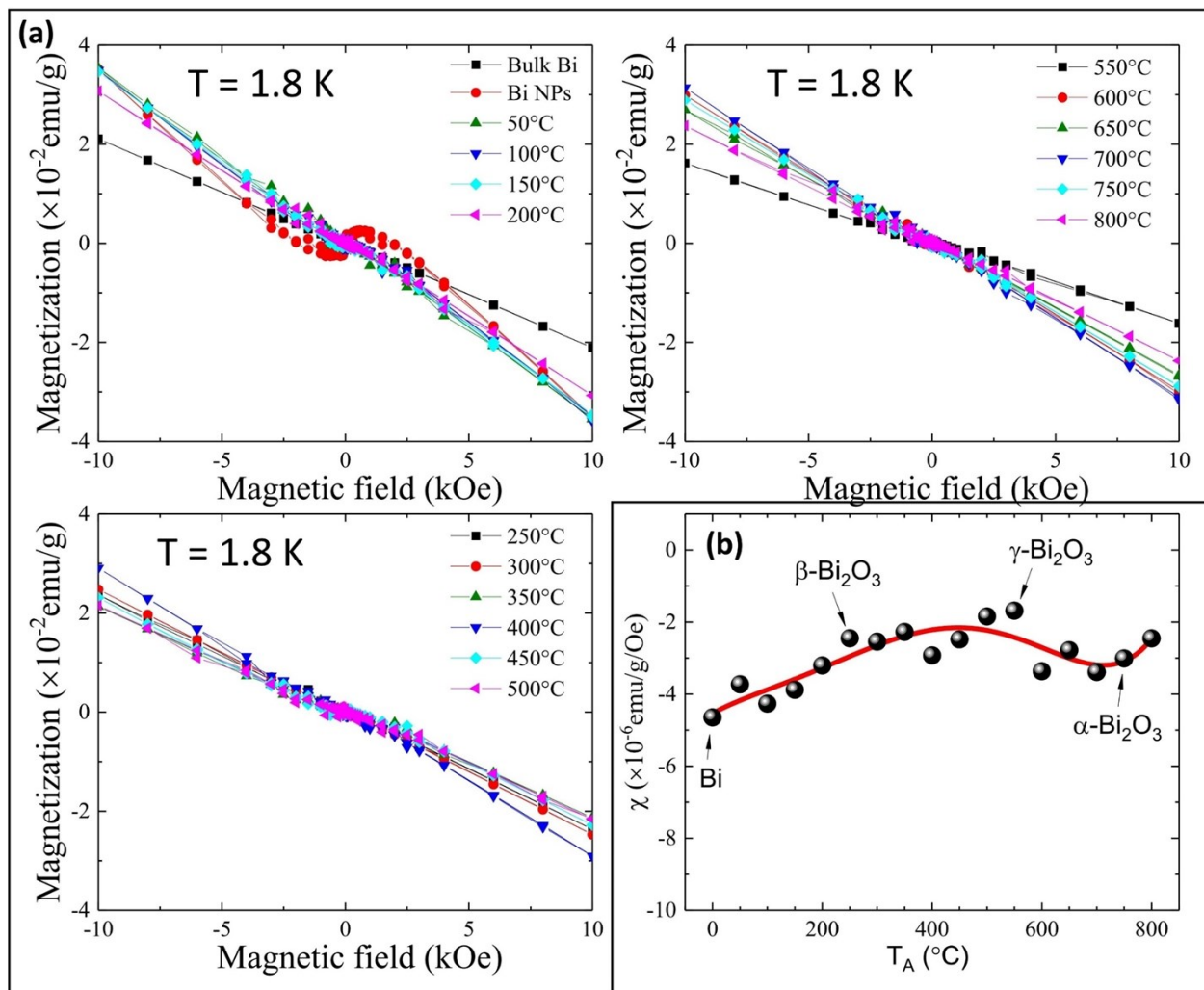
Table S1 Summary of Rietveld refined fitted parameters for bismuth phase ($\alpha=\beta=90°$, $\gamma=120°$, $x = y = 0$, space group $R\overline{3}m$, No. 166).

Parameters	Bi	50 °C	100 °C	150 °C	200 °C
a = b (Å)	4.4881(4)	4.4853(5)	4.4862(4)	4.4876(4)	4.4897(5)
c (Å)	11.7048(5)	11.6884(6)	11.7009(6)	11.7055(5)	11.6965(13)
V (Å³)	204.19(3)	203.64(3)	203.95(3)	204.15(2)	204.19(2)
z	0.2327(1)	0.2330(1)	0.2329(1)	0.2330(1)	0.2316(2)
wR(%)	1.144	1.14	1.15	1.21	0.86
GOF(%)	3.13	3.33	3.32	3.27	2.36
Wt. fraction (%)	100	100	100	88.3(2)	18.8(1)

Table S2 Summary of Rietveld refined fitted parameters for β-Bi$_2$O$_3$ phase (α=β=γ=90°; O(2): x=0, y=0.5; space group $P\bar{4}2_1c$, No.114).

Parameters		150 °C	200 °C	250 °C	300 °C	350 °C	400 °C	450 °C	500 °C
$a = b$ (Å)		7.6403(6)	7.6456(1)	7.6448(1)	7.6416(1)	7.64143(6)	7.6424(1)	7.6436(1)	7.8947(18)
c (Å)		5.5577(6)	5.5645(1)	5.5653(1)	5.56764(4)	5.56709(4)	5.5649(1)	5.56456(5)	5.3697(19)
V (Å^3)		324.43(5)	325.27(1)	325.26(1)	325.117	325.07	325.03(1)	325.11(1)	334.68(12)
	x	0.0134	0.0169	0.0166	0.0173	0.0179	0.0182	0.0176	0.0178
Bi(1)	y	0.2601	0.2540	0.2550	0.2543	0.2539	0.2552	0.2549	0.2537
	z	0.2522	0.2403	0.2399	0.2375	0.2378	0.2364	0.2373	0.2376
	x	0.4510	0.3047	0.3044	0.2914	0.2966	0.2818	0.2896	0.2949
O(1)	y	0.3312	0.3105	0.3103	0.3132	0.3144	0.3148	0.3202	0.3250
	z	0.1571	0.0295	0.0230	0.0121	0.0220	0.0121	0.0120	0.0287
O(2)	z	0.3879	0.3843	0.3863	0.4036	0.41432	0.3833	0.3960	0.4184
wR(%)		1.21	0.86	0.89	1.76	1.94	1.92	2.38	2.14
GOF(%)		3.27	2.36	2.42	3.82	4.41	3.59	6.28	5.72
WF (%)		11.7(3)	81.2(1)	100	90.8(3.8)	95.4(3.8)	66.5(4.2)	66.4(3.2)	1.12(8)
Bi(1)		0.91(12)	0.90(1)	0.828(8)	0.788(16)	0.965(19)	0.824(26)	0.905(22)	1
O(1)		1	1	1	1	1	1	1	1
O(2)		1	1	0.95(2)	0.829(32)	0.939(33)	0.713(46)	0.822(45)	1

Table S3 Summary of Rietveld refined fitted parameters for γ-Bi_2O_3 phase (α=β=γ=90°; Bi(2): x=y=z=0; O(2) and O(3): x=y=z; space group *I*23, No. 197).

Parameters		300 °C	350 °C	400 °C	450 °C	500 °C	550 °C	600 °C	650 °C	700 °C
a = b (Å)		10.1145(4)	10.1335(34)	10.1040(4)	10.1087(1)	10.0994(1)	10.1114(1)	10.1105(1)	10.1080(1)	10.1062(2)
V (Å³)		1034.8(1)	1041(1)	1031.53(11)	1032.98(4)	1030.11(3)	1033.82(3)	1033.51(2)	1032.75(2)	1032.2(1)
	x	0.8287	0.8244	0.8308	0.8262	0.8247	0.8244	0.8232	0.8234	0.8259
Bi(1)	y	0.6868	0.6801	0.6854	0.6817	0.6818	0.6801	0.6803	0.6808	0.6828
	z	0.9822	0.9881	0.9865	0.9877	0.9868	0.9881	0.9880	0.9872	0.9875
	x	0.8112	0.8690	0.8170	0.8434	0.8538	0.8690	0.8682	0.8650	0.8362
O(1)	y	0.7655	0.7661	0.7736	0.7420	0.7487	0.7661	0.7537	0.7500	0.7116
	z	0.5217	0.4884	0.4810	0.5143	0.4856	0.4884	0.4836	0.4914	0.5431
O(2)	x	0.8182	0.8093	0.8422	0.8311	0.8057	0.8093	0.8097	0.8018	0.8292
O(3)	x	0.1284	0.1624	0.1453	0.2019	0.1426	0.162	0.1487	0.1384	0.1951
wR(%)		1.76	1.94	1.92	2.38	2.14	2.460	2.63	2.65	4.35
GOF(%)		3.82	4.41	3.59	6.27	5.72	4.71	5.26	4.64	7.98
Wt. fraction (%)		7.1(1.3)	0.5(0.1)	14.6(5.0)	32.6(3.9)	98.3(0.1)	100	99.5(6.0)	92.2(1)	21*
Bi(1)		0.98(9)	1	0.995(171)	0.872(53)	0.927(29)	0.9989(4)	0.975(29)	0.941	1
Bi(2)		0.819(104)	1	0.774(146)	0.825(43)	0.741(20)	0.943(8)	0.837(33)	0.733(5)	1
O(1)		1	1	1	1	1	1.0104(17)	0.993(33)	0.998(13)	1
O(2)		1	1	0.841(202)	0.676(86)	0.668(35)	0.861(29)	0.965(38)	0.761(19)	1
O(3)		1	1	1	1	0.766(42)	1.08(4)	1	1	1

Table S4 Summary of Rietveld refined fitted parameters for α-Bi$_2$O$_3$ phase (α=β=90°, space group $P2_1/c$, No. 14).

Parameters		300 °C	350 °C	400 °C	450 °C	500 °C	600 °C	650 °C	700 °C	750 °C	800 °C
a (Å)		5.7763(55)	5.7773(45)	5.7779(8)	5.7768(32)	5.7856(61)	5.7792(15)	5.7776(6)	5.7774(2)	5.7776(3)	5.7775(4)
b (Å)		8.0695(7)	8.0710(5)	8.0638(1)	8.0712(6)	8.0507(6)	8.0660(3)	8.0655(1)	8.0663(1)	8.0654(1)	8.0639(1)
c (Å)		7.4175(86)	7.4170(7)	7.4164(13)	7.4177(52)	7.4146(94)	7.4156(24)	7.4183(9)	7.4185(4)	7.4178(5)	7.4173(7)
β (deg.)		112..98(2)	112.92(1)	112.981(3)	113.01(1)	112.96(2)	112.995(5)	112.982(2)	112.977(1)	112.978(1)	112.977(1)
V (Å^3)		318.31(4)	318.39(3)	318.12(1)	318.33(4)	318.00(3)	318.21(2)	318.25(1)	318.29(1)	318.24(1)	318.15(1)
	x	0.5230	0.5267	0.5283	0.5283	0.5283	0.5283	0.5283	0.5241	0.5249	0.5223
Bi(1)	y	0.1842	0.1893	0.1847	0.1847	0.1847	0.1847	0.1847	0.1847	0.1832	0.1846
	z	0.3580	0.3686	0.3656	0.3656	0.3656	0.3656	0.3656	0.3624	0.3593	0.3579
	x	0.0395	0.0223	0.0352	0.0352	0.0352	0.0352	0.0352	0.0400	0.0389	0.0393
Bi(2)	y	0.0424	0.0336	0.0423	0.0423	0.0423	0.0423	0.0423	0.0419	0.0426	0.0428
	z	0.7755	0.7784	0.7739	0.7739	0.7739	0.7739	0.7739	0.7753	0.7751	0.7755
	x	0.7855	0.6927	0.7624	0.7624	0.7624	0.7624	0.7624	0.7824	0.7768	0.6927
O(1)	y	0.3225	0.4299	0.3094	0.3094	0.3094	0.3094	0.3094	0.3136	0.2919	0.4299
	z	0.7025	0.5839	0.7044	0.7044	0.7044	0.7044	0.7044	0.7206	0.7304	0.5839
	x	0.2895	0.3106	0.2895	0.2895	0.2895	0.2895	0.2895	0.2438	0.2783	0.3106
O(2)	y	0.0346	0.0688	0.0346	0.0346	0.0346	0.0346	0.0346	0.0347	0.0467	0.0688
	z	0.1292	0.2031	0.1292	0.1292	0.1292	0.1292	0.1292	0.1345	0.1340	0.2031
	x	0.2993	0.2712	0.2993	0.2993	0.2993	0.2993	0.2993	0.2648	0.2712	0.2712
O(3)	y	0.0629	0.0633	0.0629	0.0629	0.0629	0.0629	0.0629	0.0461	0.0605	0.0633
	z	0.5004	0.5282	0.5089	0.5089	0.5089	0.5089	0.5089	0.4815	0.4987	0.5282

wR(%)	1.76	1.94	1.92	2.38	2.14	2.63	2.65	4.35	7.31	6.73
GOF(%)	3.82	4.41	3.59	6.27	5.72	5.26	4.64	7.98	13.89	12.36
Wt. fraction (%)	2.1(1)	4.5(1)	18.9(2.2)	0.8(3)	0.60(5)	0.45(4)	7.8(1)	70*	76*	75*
Bi(1)	1	1	0.858(49)	1	1	1	1	0.698(21)	1	0.821(47)
Bi(2)	1	0.931(6)	0.818(46)	1	1	1	1	0.681(21)	1	0.808(46)
O(1)	1	1	1	1	1	1	1	0.771(36)	0.592(36)	0.668(82)
O(2)	1	1	1	1	1	1	1	0.792(31)	1	1
O(3)	1	1	1	1	1	1	1	1	1	1

Table S5 List of 2θ values obtained from x-Bi$_2$O$_3$ is compared with reported δ-Bi$_2$O$_3$ (a = 5.4984 Å; Space group: $Fm\bar{3}m$ (No. 225); Lattice cites: Bi(0,0,0), O1(1/4,1/4,1/4), O2(0.324,x,x)).[2]

x-Bi$_2$O$_3$				δ-Bi$_2$O$_3$		
No.	2θ (deg.)	No.	2θ (deg.)	No.	2θ (deg.)	I
1	9.39	15	26.89	1	14.96	100
2	11.531	16	27.78	2	17.29	8.99
3	13.334	17	28.605	3	24.55	85.29
4	14.926*	18	29.052	4	28.87	66.25
5	16.17	19	29.41	5	30.18	8.32
6	16.368	20	31.66	6	34.99	6.63
7	17.484	21	32.04	7	38.25	12.24
8	21.202	22	32.438	8	39.28	16.51
9	22.253	23	33.444	9	43.21	13.95
10	22.983	24	33.861	10	45.98	8.26
11	23.259	25	40.321	11	50.33	4.16
12	23.932	26	41.509	12	52.81	13.23
13	24.226	27	48.14	13		
14	26.058			14		

*Most intense peak

Table S6 Summary of estimated grain size from the most intense PXRD peak and the fitted parameters to the histogram obtained from SEM images of Bi and the air annealed samples.

$T_A(°C)$	Grain size (nm)					SEM	
	Bi	β-Bi$_2$O$_3$	γ-Bi$_2$O$_3$	α-Bi$_2$O$_3$	x-Bi$_2$O$_3$	$<d>$ (nm)	σ
0	28	…..	…...	…...	…...	34.0(1)	0.30(4)
50	20	…..	…..	…..	…..	30.6(8)	0.21(4)
100	20	…..	…..	…..	…..	27.6(5)	0.25(3)
150	23	32	…..	…..	…..	27.4(4)	0.18(2)
200	6	46	…..	…..	…..	33.9(5)	0.18(2)
250	…..	39	…..	…..	…..	31.8(4)	0.21(2)
300	…..	62	59	125	…...	40.5(6)	0.33(2)
350	…..	62	61	115	…..	41.7(7)	0.30(2)
400	…..	65	81	252	…..	52.9(1)	0.25(3)
450	…..	72	72	136	…..	61.1(1)	0.278(2)
500	…..	52	67	162	…..	64.5(6)	0.269(9)
550	…...	…...	90	159	…..	90(1)	0.25(2)
600	…..	…..	105	192	…..	131(3)	0.27(3)
650	…..	…..	125	227	…..	219.5(5)	0.29(4)
700	…..	…..	93	207	53	319(8)	0.303(34)
750	…..	…..	…..	234	86	319(3)	0.27(1)
800	…..	…..	…..	221	104	470(3)	0.275(5)

Table S7 Summary of fitted values of Raman scattering frequencies obtained from Bi and the air annealed samples.

No.	Bi	50°C	100°C	150°C	200°C	250°C	300°C	350°C	400°C	450°C	500°C	550°C	600°C	650°C	700°C	750°C	800°C
1	90	96	97	97	94	90	90	93	91	90	81	81	82	82	…..	54	…..
2	111	111	110	111	110	109	109	110	108	103	88	89	93	89	58	57	…..
3	114	125	123	123	125	127	127	127	127	114	111	111	109	111	68	68	69
4	138	136	145	140	143	142	142	141	142	127	126	125	124	126	85	84	85
5	188	182	178	178	184	161	161	155	159	142	141	141	140	142	95	94	95
6	317	315	315	314	315	234	232	232	185	157	153	157	151	159	104	104	104
7	329	324	334	328	329	267	246	262	207	186	198	206	185	186	121	120	120
8	473	465	463	466	466	316	274	315	212	205	255	257	211	205	140	140	140
9	481	482	482	…..	482	322	316	320	232	212	272	281	258	257	153	153	153
10	584	574	586	583	573	468	319	465	270	270	317	312	281	280	185	185	185
11	619*	612*	627*	623*	611*	472	467	467	316	316	359	344	313	313	211	211	211
12						591	502	482	320	320	382	381	334	338	254*	255*	254*
13						628*		505	450	450	438	436	380	380	282	281	281
14								606	467	468	482*	448	434	434	314	314	314
15								638*	471*	475*	516	481*	448	448	330	333	334
16									526	529	530	494	482*	482*	412	412	412
17									571*	569*	566*	528	518	500	436	434	438
18									616	606	621	567*	530	529	449	448	449
19									637	630	633	614	566*	567*	464	461	465
20												628	617	619	531	536	536
21													630	632	617*	622*	623*

*Not assigned to any reported vibration mode.

Table S8 Summary of fitted values of FWHM of various phonon modes obtained from Bi and the air annealed samples.

No.	Bi	50°C	100°C	150°C	200°C	250°C	300°C	350°C	400°C	450°C	500°C	550°C	600°C	650°C	700°C	750°C	800°C
1	23	26	27	28	22	14	14	18	15	16	9	10	10	9	…..	2	…..
2	9	13	10	9	14	31	28	18	28	20	13	15	12	13	4	2	…..
3	28	15	25	19	13	11	11	13	11	25	25	23	16	18	4	5	5
4	49	45	35	35	40	21	21	12	19	11	10	10	13	10	9	7	7
5	31	32	31	33	28	17	13	24	14	15	12	14	9	13	9	9	9
6	23	20	26	25	21	16	12	11	7	16	45	23	20	22	5	5	5
7	7	55	66	58	54	49	11	34	7	7	24	14	8	27	9	8	8
8	37	30	35	47	32	16	37	16	8	6	22	27	12	18	7	7	7
9	5	6	6	…..	3	51	14	49	7	8	33	28	25	25	10	10	10
10	65	35	59	46	45	21	40	40	34	36	49	36	25	34	11	11	11
11	49*	60*	49*	47*	58*	52	28	17	15	16	38	54	32	32	13	13	13
12						44*	41	6	49	54	28	30	66	53	12*	13*	12*
13								49	23	22	27	12	24	31	32	29	29
14								51	18	17	5*	11	11	12	20	22	22
15								29*	41*	39*	46	5*	18	15	35	31	31
16									31	33	31	26	1*	5*	19	21	21
17									11*	18*	25*	34	41	30	20	19	24
18									29	5	12	22*	32	32	17	17	17
19									27	32	20	16	22*	21*	25	27	24
20												24	15	18	27	23	23
21													22	19	21*	*30	23*

*Not assigned to any reported vibration mode.

Table S9 Summary of fitted values of integrated area (I. A.) of various phonon modes obtained from Bi and the air annealed samples.

No.	Bi	50°C	100°C	150°C	200°C	250°C	300°C	350°C	400°C	450°C	500°C	550°C	600°C	650°C	700°C	750°C	800°C
1	4552	14035	20081	17104	19660	46945	206968	139772	264039	180037	17648	83481	63696	68380	…..	28	…..
2	624	299	2150	1607	9050	134851	401264	109195	431953	82315	17944	78898	42987	47335	68	38	…..
3	9177	5451	17035	7684	14443	36557	161052	97849	222184	157613	36421	147044	51361	59361	496	2274	1900
4	18383	16987	10470	8332	17502	35010	104119	18981	105374	133050	20805	128977	116978	118523	66614	77643	58608
5	1651	1617	2259	2163	1426	14208	29370	35388	43045	57586	7654	78006	21827	50594	101772	176890	136177
6	1395	9099	15980	8658	23729	2585	8892	2461	3412	39815	61937	76541	52294	50657	9871	18612	13586
7	89	9065	7902	6683	10219	12081	2599	5541	2510	3324	4747	7588	7726	9953	151734	258812	199632
8	1463	1801	736	1340	4289	177490	28773	238206	5959	1562	22523	244743	23168	12547	38621	96096	75701
9	121	257	318	…..	111	87607	402463	235599	3092	6902	45110	173174	134700	160425	78913	174090	139057
10	4103	1522	7458	2727	3693	36623	480832	88008	43410	62841	114747	385620	117383	212848	120003	246495	193564
11	1233*	5183*	3677*	2612*	7652*	32015	267898	24861	615687	408868	28486	348462	218755	225325	209476	446501	355856
12						6236*	16512	2759	714826	456733	19358	106712	286150	320767	11108*	23431*	13603*
13								16752	58078	52460	2253	1435	31166	103351	411103	832704	651709
14								4282	100257	58189	1436*	4063	4732	1649	590807	1023230	790509
15								3538*	167188*	77220*	47891	1195*	49501	4580	342036	485860	351346
16									54251	116203	100737	41940	3683*	4682*	73066	199766	145419
17									1125*	7526*	16691*	633061	78699	52044	128275	251968	281265
18									9583	347	754	61076*	296904	526159	296805	669892	537159
19									12142	11234	3786	5137	35779*	43960*	127604	225167	115444
20											29613	4485		16841	100123	165231	112938
21													15412	14970	30168*	21545*	11183*

*Not assigned to any reported vibration mode.

Table S10 Summary of fitted values of bandgap energy obtained from high-resolution Bi 4f XPS spectra of Bi, β-Bi$_2$O$_3$ (top), and γ- and α-Bi$_2$O$_3$ (bottom).

Sample	Bi^{3+} 4f$_{7/2}$			BiCOx			Bi^{3+} 4f$_{5/2}$		
	B.E.	A	FWHM	B.E.	A	FWHM	B.E.	A	FWHM
Bi	158.77	16229	1.85	161.60	13694	3.91	163.59	16441	1.85
β-Bi$_2$O$_3$	158.51	13451	1.94	161.19	23526	3.59	163.44	33171	1.94

Sample	Bi^{3+} 4f$_{7/2}$			S			Bi^{3+} 4f$_{5/2}$			S		
	B.E.	A	FWHM	B.E.	A	FWHM	B.E.	A	FWHM	B.E.	A	FWHM
γ-Bi$_2$O$_3$	158.86	34873	1.90	160.84	19040	2.10	164.19	23286	1.90	166.11	13555	2.10
α-Bi$_2$O$_3$	158.92	27262	1.80	160.37	21188	1.86	164.27	19068	1.80	165.69	14822	1.86

Table S11 Summary of fitted values of bandgap energy obtained from high-resolution O1 s XPS spectra of Bi, β-, γ- and α-Bi$_2$O$_3$.

Sample	Bi–O			OH$^-$						O–C		
	B.E.	A	FWHM	B.E.	A	FWHM	B.E.	A	FWHM	B.E.	A	FWHM
Bi	530.16	5462	2.84	…..	…..	…..	531.82	2515	2.85	533.81	5390	3.21
250°C	529.97	3716	2.67	…..	…..	…..	531.95	1534	2.9	533.0	13527	3.30
550°C	529.76	4640	1.70	530.89	4640	1.70	531.74	1715	2.79	…..	…..	…..
700°C	530.19	7679	2.17	531.25	7679	2.17	531.79	2145	2.3	…..	…..	…..

Table S12 Summary of fitted values of bandgap energy obtained from high-resolution C1 s XPS spectra of Bi, β-, γ- and α-Bi_2O_3.

Sample	C-C		C-O-C		O-C=O		C-Bi		?		
	B.E.	A	B.E.	A	B.E.	A	B.E.	A	B.E.	A	FWHM
Bi	284.8	1924	286.33	876	288.01	1228	289.19	1688	291.97	174	1.82
250°C	284.8	513	286.10	385	287.64	756	289.33	1788	292.50	385	2.01
550°C	284.8	2099	286.69	1220	288.49	808	289.66	237	…..	…..	1.87
700°C	284.8	2074	286.20	1378	288.61	839	290.00	454	…..	…..	1.83

Table S13 Summary of fitted parameters to PL spectra of Bi and the air annealed samples.
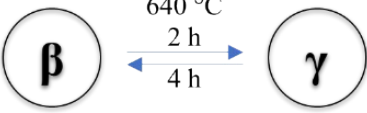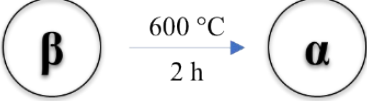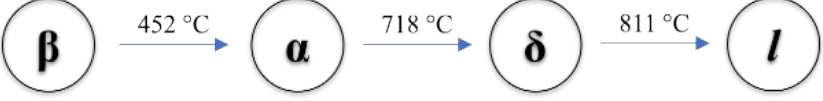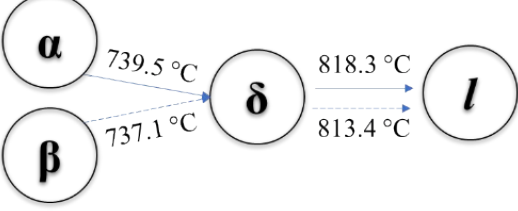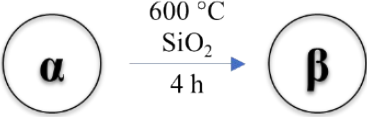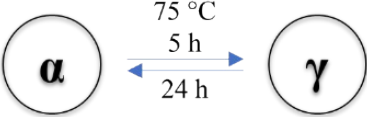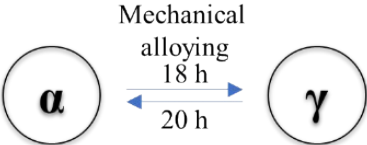
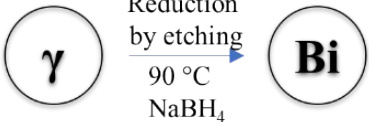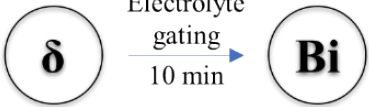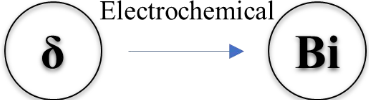| Parameters	Bi	50°C	100°C	150°C	200°C	250°C	300°C	350°C	400°C	450°C	500°C	550°C	600°C	650°C	700°C	750°C	800°C
	382	393	399	396	381	399	408	404	401	384	404	394	428	413	408	409	406
Centre	534	482	486	485	504	551	555	515	525	531	477	487	514	498	500	486	482
(nm)	593	586	586	583	593	595	589	585	588	588	587	588	588	585	584	582	585
	699	699	697	696	695	698	689	701	699	699	693	701	696	694	698	695	698
	36	43	54	58	45	50	84	55	76	16	39	57	76	73	67	66	58
FWHM	91	108	128	93	94	113	92	129	130	90	87	115	112	112	93	114	107
(nm)	40	61	61	59	38	37	61	67	58	66	59	61	64	64	60	59	63
	126	121	125	129	113	135	134	126	121	123	129	120	128	128	126	133	124
	81	194	396	619	111	159	1835	533	572	33	141	259	2345	2159	1300	1853	1350
Intensity	584	653	1183	985	484	3614	10052	2799	2135	762	781	912	6702	7341	1389	5046	3088
(Normalized)	235	2406	2574	2770	286	258	5665	4513	1051	1933	3904	1657	4155	8285	4996	10810	9810
	6236	15154	16039	16324	4596	11039	37503	27231	9383	13334	19307	11936	22148	41943	27617	58359	49769
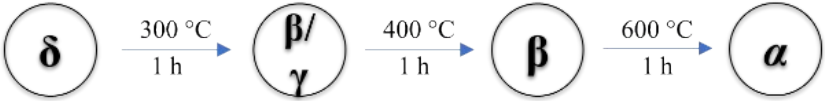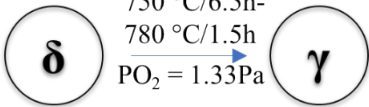
Table S14 Summary of CIE (X, Y) coordinates and CCT values obtained from PL spectra of pure and the air annealed Bi nanoparticles (left) and ingot (right).

	Annealed Bi NPs				Annealed Bi ingots		
Sample	CIE		CCT (K)	Sample	CIE		CCT (K)
	x	y			x	y	
Bi	0.4521	0.4048	2766	Bi	0.3215	0.3731	5915
50 °C	0.506	0.3955	2065	100 °C	0.3279	0.4053	5655
100 °C	0.4905	0.3903	2178	200 °C	0.3264	0.3913	5713
150 °C	0.5019	0.3932	2087	250 °C	0.3104	0.3035	6905
200 °C	0.4604	0.366	2333	300 °C	0.3454	0.3604	5018
250 °C	0.4291	0.4401	3406	400 °C	0.2866	0.2968	8982
300 °C	0.4796	0.445	2693	500 °C	0.2944	0.2997	8200
350 °C	0.4815	0.4098	2418	600 °C	0.3206	0.3195	6129
400 °C	0.4315	0.3943	3012	700 °C	0.337	0.341	5301
450 °C	0.4871	0.4204	2430				
500 °C	0.5006	0.3879	2063				
550 °C	0.4759	0.3819	2274				
600 °C	0.3989	0.3775	3535				
650 °C	0.439	0.385	2805				
700 °C	0.5014	0.3966	2115				
750 °C	0.4895	0.3926	2205				
800 °C	0.4949	0.3946	2164				

Table S15 Summary of various phase transformation reported in the literature.

Phase Transformation	Description and Reference
Bi $\xrightarrow[\text{12 h}]{\text{350 °C}}$ Nanowire (2 -1 0) → δ $\xrightarrow[\text{12 h}]{\text{350 °C}}$ δ/α; Bi → Film (2 0 2) → α; Bi → Film (1 0 -2) → β	Oxidation of Bi in the air leads to the formation of α-, β-, and δ-Bi_2O_3 because of the coherent relationship between Bi and Bi_2O_3. Heating rate: 1 °C/min.[3-5]
Bi $\xrightarrow[\text{14-18 h}]{\text{200-220 °C}}$ β	Thermal oxidation of Bi nanotube array leads to the formation of β-Bi_2O_3 nanotube array.[6]
Bi $\xrightarrow[\text{2 h}]{\text{300 °C}}$ β $\xrightarrow[\text{2 h}]{\text{500 °C}}$ γ	The anodic bismuth trioxide layers were prepared via anodization of vacuum deposited Bi film in a citric acid-based electrolyte.[7]
Bi $\xrightarrow[\text{4 h}]{\text{150-250 °C}}$ β/α $\xrightarrow[\text{4 h}]{\text{300 °C}}$ α	Thermal oxidation induced phase transformation of Bi thin film. Heating rate: 1 °C/min.[8]
Bi $\xrightarrow[\text{5 h}]{\substack{\text{Multistep-slow} \\ \text{Oxidation up to} \\ \text{500 °C}}}$ Bi/α/β/δ $\xrightarrow[\text{10 h}]{\substack{\text{Fast-oxidation} \\ \text{750 °C}}}$ δ	A template heat-treatment induced conversion of Bi nanowire array (diameter 60 nm) to Bi-Bi_2O_3 core-shell nanowires and Bi_2O_3 nanotubes (diameter 75 nm).[9]
Bi $\xrightarrow[\text{30 min}]{\text{200-300 °C}}$ β $\xrightarrow[\text{30 min}]{\text{400-600 °C}}$ α $\xrightarrow[\text{30 min}]{\text{700-750 °C}}$ γ	Structural evolution of Bi_2O_3 prepared by thermal oxidation of Bi nanoparticles in the air. Heating and cooling rate: 5 and 10°C/min.[10]
Bi $\xrightarrow[\text{2 h}]{\text{250 °C}}$ β $\xrightarrow[\text{2 h}]{\text{550 °C}}$ γ $\xrightarrow[\text{2 h}]{\text{750 °C}}$ α/x	**Current work:** The air annealed Bi nanoparticles leads to the structural evolution of Bi_2O_3.

Diagram	Description
$\beta \xrightarrow[\text{4 h}]{\substack{640\ ^\circ\text{C} \\ 2\ \text{h}}} \gamma$	Bi_2O_3-$BiFeO_3$ Glass-ceramic sample[11]
$\beta \xrightarrow[\text{2 h}]{600\ ^\circ\text{C}} \alpha$	Impact of annealing in the air on phase transformation from β-Bi_2O_3 nanotube (diameter 5.5 nm) to α-Bi_2O_3 microcrystal (800 nm).[12]
$\beta \xrightarrow{452\ ^\circ\text{C}} \alpha \xrightarrow{718\ ^\circ\text{C}} \delta \xrightarrow{811\ ^\circ\text{C}} l$	The solid-state transition of β-Bi_2O_3 nanoparticles to bulk-phase evaluated using in situ XRD.
α (739.5 °C), β (737.1 °C) $\rightarrow \delta \xrightarrow[\text{813.4 °C}]{818.3\ ^\circ\text{C}} l$	The size effect (nanowire diameters: 10 nm β-Bi_2O_3, 100 nm α-Bi_2O_3) for δ to liquid (l) phase transition but not the α or β to δ phase transition in nanoscale.[13]
$\alpha \xrightarrow[\text{4 h}]{\substack{600\ ^\circ\text{C} \\ \text{SiO}_2}} \beta$	Bi_2O_3/Bi_2SiO_5 fabricated via a facile one-step synthesis using $Bi(NO_3)_3$ and nano-SiO_2 as precursors.[14]
$\alpha \xrightarrow[\text{24 h}]{\substack{75\ ^\circ\text{C} \\ 5\ \text{h}}} \gamma$	Rod-like α-Bi_2O_3 and tetrahedral γ-Bi_2O_3 particles were fabricated by a facile solution crystallization method without any surfactants and/or templates.[15]
$\alpha \xrightarrow[\text{20 h}]{\substack{\text{Mechanical} \\ \text{alloying} \\ 18\ \text{h}}} \gamma$	Polymorphs phase transformation of Bi_2O_3 nanoparticles by the mechanical alloying method.[16]

δ →(300 °C, 1 h)→ β/γ →(400 °C, 1 h)→ β →(600 °C, 1 h)→ α	Thermal oxidation of the nanocrystalline δ-Bi_2O_3 thin-film.[17]
γ →(Reduction by etching, 90 °C, $NaBH_4$)→ Bi	γ-Bi_2O_3 tetrahedra (built up of ultra-thin nanosheets via layer-by-layer self-assembly) were etched using $NaBH_4$ at 90 °C resulting in the formation of Bi nanoparticles.[18]
δ →(Electrolyte gating, 10 min)→ Bi	Reduction of δ-Bi_2O_3 to Bi film using electrolyte gating for 10 min.[19]
δ →(Electrochemical)→ Bi	Electrochemical reduction of δ-Bi_2O_3 to granular Bi thin film.[20]
δ →(750 °C/6.5h- 780 °C/1.5h, $PO_2 = 1.33$ Pa)→ γ	Annealing of δ-Bi_2O_3 in a dynamic vacuum (P = 1.33 Pa) initially at 750 °C for 6.5 h and then at 780 °C for 1.5 h leads to phase transformation to γ-Bi_2O_3.[21]

Notes and references

1. X. Chen, J. Dai, G. Shi, L. Li, G. Wang, and H. Yang, *J. Alloys Compd.*, 2015, **649**, 872-877.

2. J. A. H. Dreyer, S. Pokhrel, J. Birkenstock, M. G. Hevia, M. Schowalter, A. Rosenauer, A. Urakawa, W. Y. Teoh and L. Mädler, *CrystEngComm*, 2016, **18**, 2046-2056.

3. C.-C. Huang, T.-Y. Wen and K.-Z. Fung, *Mater. Res. Bull*, 2006, **41**, 110-118.

4. C. C. Huang and K. Z. Fung, *Mater. Res. Bull*, 2006, **41**, 1604-1611.

5. C. C. Huang, I. C. Leu and K. Z. Fung, *Electrochem. Solid St. Lett.*, 2005, **8**, A204.

6. B. Yang, M. Mo, H. Hu, C. Li, X. Yang, Q. Li and Y. Qian, *Eur. J. Inorg. Chem.*, 2004, **2004**, 1785-1787.

7. M. Ahila, J. Dhanalakshmi, J. C. Selvakumari and D. P. Padiyan, *Mater. Res. Express*, 2016, **3**, 105025.

8. T. P. Gujar, V. R. Shinde and C. D. Lokhande, *Appl. Surf. Sci.*, 2008, **254**, 4186-4190.

9. L. Li, Y.-W. Yang, G.-H. Li and L.-D. Zhang, *Small*, 2006, **2**, 548-553.

10. A. J. Salazar-Pérez, M. A. Camacho-López, R. A. Morales-Luckie, V. Sánchez-Mendieta, F. Ureña-Ñúñez and J. Arenas-Alatorre, *SMCSYV*, 2005, **18**, 4-8.

11. F. H. Margha, E. K. Radwan, M. I. Badawy and T. A. Gad-Allah, *ACS Omega*, 2020, **5**, 14625-14634.

12. H. Lu, B. Dong, S. Wang, L. Zhao, Z. Xu, L. Wan and J. Li, *Phys. Status Solidi*, 2012, **209**, 2157-2160.

13. Y. Qiu, M. Yang, H. Fan, Y. Zuo, Y. Shao, Y. Xu, X. Yang and S. Yang, *Mater. Lett.*, 2011, **65**, 780-782.

14. H. Lu, Q. Hao, T. Chen, L. Zhang, D. Chen, C. Ma, W. Yao and Y. Zhu, *Appl. Catal. B-Environ.*, 2018, **237**, 59-67.

15. G. Liu, S. Li, Y. Lu, J. Zhang, Z. Feng and C. Li, *J. Alloys Compd.*, 2016, **689**, 787-799.

16. S. Bandyopadhyay, S. Dutta, A. Dutta and S. K. Pradhan, *Cryst. Growth Des.*, 2018, **18**, 6564-6572.

17. H. T. Fan, S. S. Pan, X. M. Teng, C. Ye and G. H. Li, *J. Phys. D*, 2006, **39**, 1939-1943.

18. Y. Wang and Y. Li, *J. Colloid Interf. Sci.*, 2015, **454**, 238-244.

19. L. Fan, Y. Zhu, Z. Wang, S. Zhao, Z. Liu, L. Zhu, X. Wang and Q. Zhang, *Appl. Phys. Lett.*, 2019, **115**, 261601.

20. Z. He, J. A. Koza, Y.-C. Liu, Q. Chen and J. A. Switzer, *RSC Adv.*, 2016, **6**, 96832-96836.

21. L. A. Klinkova, V. I. Nikolaichik, N. V. Barkovskii and V. K. Fedotov, *Russ. J. Inorg. Chem.*, 2007, **52**, 1822-1829.